Research Article

Effect of Physicochemical Properties of Co and Mo Modified Natural Sourced Hierarchical ZSM-5 Zeolite Catalysts on Vanillin and Phenol Production from Diphenyl Ether

Anita Nur Ramadhani, Iman Abdullah, Yuni Krisyuningsih Krisnandi*

Department of Chemistry, Faculty of Mathematics and Natural Science, Universitas Indonesia, Depok-16424, Indonesia

Solid Inorganic Framework Laboratory, Department of Chemistry, Faculty of Mathematics and Natural Science, Universitas Indonesia, Depok-16424, Indonesia

Abstract

The conversion of lignocellulose biomass to value-added chemicals is challenging. In this paper, the conversion process of diphenyl ether (DPE) as a model lignin compound to phenol and vanillin compounds involved a bifunctional catalyst in reaching the simultaneous one-pot reaction in mild conditions with a high yield product. The catalysts used in this conversion are hierarchical ZSM-5 zeolites and their cobalt oxide and molybdenum oxide impregnated derivate. The ZSM-5 zeolites were synthesized using alternative precursors from natural resources, i.e., Indonesian natural zeolite and kaolin. The physicochemical properties of the catalysts were determined with various characterization methods, such as: X-ray Diffraction (XRD), Fourier Transform Infra Red (FT-IR), Scanning Electron Microscope - Energy Dispersive X-ray (SEM-EDX), X-ray Fluorescence (XRF), Surface Area Analyzer (SAA), and NH_3-Temperature Programmed Desorption (NH_3-TPD). The catalytic activity on conversion of DPE substrates showed that the MoO_x/HZSM-5 produced the highest %yield for phenol and vanillin products; 31.96% at 250 °C and 7.63% at 200 °C, respectively. The correlation study between the physicochemical properties and the catalytic activity shows that the dominance of weak acid (>40%) and mesoporosity contribution (pore size of ~ 9 nm) play roles in giving the best catalytic activity at low temperatures.

1. Introduction

The main challenge in fine chemical industrial development is the replacement of fossil resources with sustainable resources. The utilization of lignocellulosic biomass has recently shown a rapid development due to being the only renewable resource of organic carbon in nature, which provides advantages in value-added chemical production [1]. The chemical structure of lignin has many aromatic structures with specific ether bonding for each monolignol [2]

* Corresponding Author.
  Email: yuni.krisnandi@sci.ui.ac.id (Y.K. Krisnandi)

that become a source of high-value compounds, such as vanillin and phenol [3]. However, regarding the complexity of the lignin structure, the conversion mechanism becomes unclear. The simplification of the complexity of the lignin fraction can be seen in several existing model compounds, such as diphenyl ether (DPE) as a representative of 4-O-5 bonding, phenethyl phenyl ether (PPE) as representative of β-O-4 bonding and benzyl phenyl ether (BPE) as representative of α-O-4 bonding [4].

ZSM-5 as a heterogeneous catalyst is commonly used in biomass conversion because of its porosity, leading to a good shape selectivity of products and good thermal stability [5]. Deepa et al. reported that the presence of conventional HZSM-5 shows that biomass depolymerization produced around 60% of aromatic monomers [6]. Hereafter, several modifications in ZSM-5, such as modification of the pores into hierarchical pores and the addition of metal oxides, have shown to increase the catalytic effectiveness in biomass conversion, especially to improve the selectivity of the reaction product.

CoO_x/HZSM-5 in the pyrolysis reaction produced the highest distribution yield for monocyclic aromatic compounds [7] and facilitated the conversion of bio-oil into phenolic and guaiacol products with the increasing selectivity of 9.2% and 15.3% compared with the non-catalyzed reaction [8]. Also reported, the pyrolysis reaction's selectivity to produce phenolic derivative products facilitated by Mo modified ZSM-5 was 30% [9]. The impregnation of the Mo oxide on ZSM-5 produced monocyclic aromatic with the highest yield, and selectivity was 84.5% in fast pyrolysis reaction [10]. Hydrogenolysis of aryl ether bond over heterogenous cobalt-based catalysts also show the 97% selectivity of C−O bond ruptured products was achieved from DPE model lignin compound, with the major product were phenol and benzene [11]. Also reported that Mo-based catalysts leading the effective hydrodeoxygenation of biomass-derived oxygenates, such as lignin model compounds [12,13]. Based on these several reports, it is shown that combination of acid sites in zeolite and metal oxide species, such as cobalt oxides and molybdenum oxides can effectively improve the lignin conversion.

For research purposes, the synthesis of ZSM-5 catalysts usually uses pro analyst precursors. Nonetheless, taking into account the environmental, economic, and abundances in nature, the use of natural resources as alternative precursors can be a distinct added value. It has been studied the success of zeolite synthesis from alternative resources, for example, ka-

olin [14,15], rectorite with diatomite [16], and a combination of Indonesia zeolite and kaolin [17]. In this work, the ZSM-5 catalyst was synthesized using the alternative precursor, i.e. Indonesian natural zeolite and kaolin. The as-synthesized ZSM-5 then was converted to HZSM-5, followed by modification with molybdenum and cobalt oxides to provide more active sites in the catalyst.

In this present work, we aimed to study the conversion of diphenyl ether (DPE), one of the lignin models, to more useful chemicals, such as phenolic compounds and vanillin using Mo-oxides and Co-oxides-modified HZSM-5 catalysts (MoO_x/HZSM-5 and CoO_x/HZSM-5). The correlation between physicochemical properties and activity of catalyst on DPE conversion, as well as the optimum conditions to obtain the highest %yield of vanillin and phenol are discussed.

2. Materials and Methods

2.1 Materials

Indonesian natural zeolite was from Bayat Klaten, Central Java. The kaolin used was provided by PT Aneka Kaolin Utama, Belitung Indonesia. NaOH pellet 99 %, nitric acid, hydrochloric acid, hydrogen peroxide 30%, glacial acetic acid, sodium acetate tetrahydrate, sodium bicarbonate, ethanol, trisodium citrate dihydrate, $Co(NO_3)_2.6H_2O$, NH_4NO_3, and methanol were purchased by Merck (Germany). Tetra-propylammonium hydroxide (TPAOH 40%), $(NH_4)_6Mo_7O_{24}.4H_2O$, and polydiallyldimethylammonium chloride acrylamide (PDDAM, 10 %) purchased from Sigma Aldrich, US. And the phosphoric acid (97 %) was purchased from PT. Smart Lab Indonesia.

2.2. Synthesis of Hierarchical ZSM-5 Catalyst from Natural Resources

Natural zeolite and kaolin were pre-treated with the activation, purification, fragmentation, and calcination processes following the procedure from Rohayati *et al.* [18]. The synthesis of hierarchical ZSM-5 using a molar ratio of 3 Al_2O_3: 64.35 SiO_2: 10.07 $(TPA)_2O$: 3571.66 H_2O. Fragmented Indonesia zeolite and extracted silica from kaolin as the precursors were mixed with H_2O, stirred overnight. Furthermore, TPAOH and TEOS were added dropwise into the mixture while stirring at 100 °C. Then, the pH solution was adjusted to ±11 using acetic acid glacial followed by aging for three hours. Afterward, a certain amount of PDD-AM was slowly added into the reaction

mixture at room temperature and stirred for 24 h. After stirring, the mixture was transferred into an autoclave for further crystallization at 170 °C for 144 h. The crystals were washed with H_2O and then dried in the oven at 60 °C, then calcined in the atmospheric pressure at 550 °C for five hours [19]. The as-synthesized hierarchical ZSM-5 then was named ZSM-5.

2.3. Preparation of Hierarchical HZMS-5 Catalyst

Multiple ammonium exchange was carried out using a solution of NH_4^+ 1 M at 90 °C for two hours under stirring for three repetitions. The resulting NH_4/ZSM-5 then was calcined gradually at 550 °C for 5 hours to produce H/ZSM-5 [20] and named as HZSM-5.

2.4 Preparation of Hierarchical CoO_x/ZSM-5 and MoO_x/ZSM-5 Catalysts

Catalyst modification was carried out by wet impregnation for 10 %wt metal loaded by adding 1.1313 M of $Co(NO_3)_2 \cdot 6H_2O$ or 0.0355 M of $(NH_4)_6Mo_7O_{24}.4H_2O$ into 1 gram of ZSM-5 or HZSM-5 using spraying method multiple times to form a paste [21] and left for 24 hours before it was calcined gradually at 550 °C to obtained CoO_x/ZSM-5 [22] and at 500 °C to obtained MoO_x/ZSM-5 [23]. Furthermore, the as-prepared catalysts were named CoO_x/ZSM-5, CoO_x/HZSM-5, MoO_x/ZSM-5, and MoO_x/HZSM-5.

2.5. Characterization of Catalysts

All catalysts were then characterized using XRD, FT-IR, XRF, SEM, EDS, SAA, and NH_3-TPD. The FT-IR analysis used Alpha – Bruker, while the XRD was carried out in PANalytical XPert PRO 2318 diffractometer with Cu-K radiation (λ =1.54184 Å) as the incident beam. Analysis XRF using PANanalytical epsilon1. The SEM-EDS measurement using FE-SEM JIB-4610F, Schottky electron gun robe current (200nA), electron backscatter diffraction (EBSD), cathodoluminescence (CLD). Moreover, for the surface area analyzer, use Quantachrom-Evo Surface Area and Pore Analyzer. And for the acidity properties was analyzed using NH_3-TPD Chemisorb 2750 micrometric, with the sample heated at 350 °C for 60 min under He gas (inert) as the pre-treatment, followed by the NH_3 adsorption was carried out at 100 °C for 30 minutes using NH_3 5% in He (v/v), then purged with He gas (inert) at the same temperature, for 30 minutes. Afterward, the NH_3 desorption was carried out at a temperature of 100–700 °C with an increasing speed of 10 °C/minute, then held for 15 minutes at the temperature of 700 °C, with the entire gas flow rate of 40 mL/min.

2.6. Catalytic Activity Test

The conversion reaction was performed in a batch reactor shown in Figure 1. The procedure was following Deepa *et al*. [6] and Pratama *et al*. [17] with modification. The reaction was carried out under an inert condition with 2 atm of N_2 at room temperature. The solvent was water: ethanol (1:1 v/v) mixture in a total volume of 25 mL. The amount of DPE and the catalyst added was 0.25 g and 0.125 g, respectively. The reaction was performed under a stirring condition with 500 rpm for 30 min [17]. The reaction temperature varied at 150, 200, and 250 °C.

After the reaction, the filtrate was separated and prepared for analysis with the HPLC using PG LC210 equipped with C18 column, and a mixture of methanol: distilled water (80:20) as eluent. The % conversion of DPE, and the % yield of phenol and vanillin are calculated using the standard calibration curve and determined using following equations:

$$\%DPE\ Conversion = \frac{Init.\ Substrate\ Mass(g) - Residual\ Mass\ (g)}{Substrate\ Mass\ (g)} x\ 100\%$$

(1)

$$\%Yield = \frac{Product\ Concent.\ (mg\ /\ L)\ x\ Solution\ Volume\ (L)}{Substrate\ Mass\ (g)} x100\%$$

(2)

3. Results and Discussion

3.1. Catalyst Characterizations

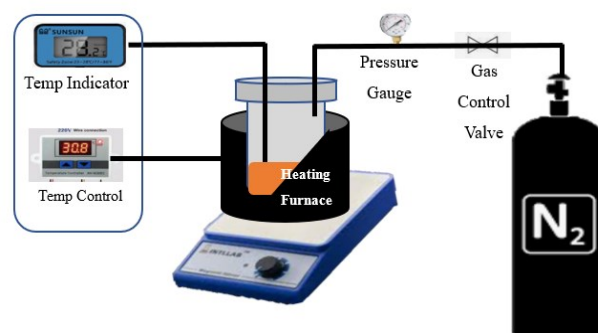Figure 2 shows the diffractogram of all as-prepared catalysts, which reveals the specific

Figure 1. Schematic diagram of DPE conversion in a batch reactor

pattern for ZSM-5 based on JCPDS 49-0657 [24] that in angel $2\theta = 7\text{-}10^0$, $22\text{-}25^0$ [25,26]. It depicts that the MFI (Mordenite Framework Inverted) as the pentasil framework was successfully synthesized. Moreover, as-synthesized ZSM-5 also has another phase as the presence of a strong peak around the angle of 26.7 which is probably the quartz phase. This due to the precursor from the natural resources, so the quartz phase of unreacted silica can be found in the material.

Furthermore, Figure 2 shows new diffraction as Co_3O_4 phase ($2\theta = 19°$, $31°$, $37°$, $45°$, $56°$, $59°$) in cobalt oxide modified catalysts referred to JCPDS No. 42–1467 [27]. The XRD patterns of Mo oxide modified catalysts also show new diffraction peaks for MoO_3 phase ($2\theta = 13°$, $23°$, $27°$, $34°$, $38°$, $46°$, $49°$, $50°$,$51°$, $53°$,$54°$, $56°$, $59°$, $64°$) as referred to JCPDS No. 05–0508 [28]. These results inform that the incorporation of Co-oxide or Mo-Oxide into ZSM-5 was done successfully.
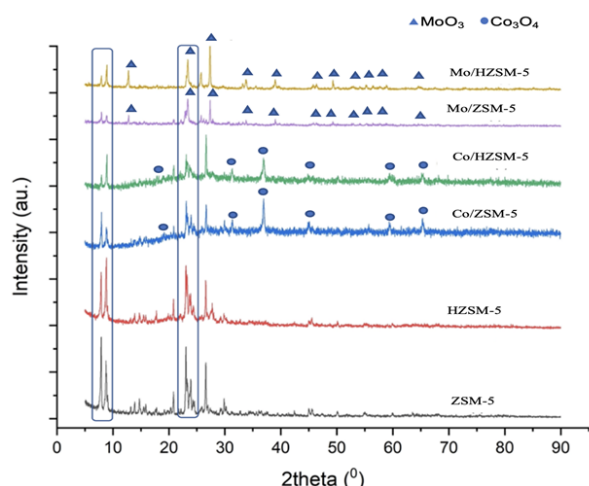

Figure 2. XRD patterns of as-prepared and modified ZSM-5 catalysts

FT-IR spectra for the as-prepared catalysts can be seen in Figure 3. In the wavenumber around 3500 cm^{-1} a broad band appeared in all spectra, which is assigned to water molecules that are hydrogen-bonded to silanol groups (Si-OH) from the surface of ZSM-5 [22,29]. There were differences in its intensity in the spectra of Mo and Co impregnated ZSM-5 and HZSM-5, indicating the closure of the area due to the metal impregnation process in ZSM-5 zeolite. Furthermore, the other typical peaks of the MFI structure of ZSM-5 zeolite are shown as the absorption band of asymmetric stretching from the T−O at 1075-1250 cm^{-1}, symmetric stretching of T−O at 820-650 cm^{-1}, and at 650-500 cm^{-1} assigned as pentasil double five rings [29].

Additional peaks appear in the fingerprint area between 1000-500 cm^{-1} for all the as-prepared catalysts, indicating the presence of metal oxide in ZSM-5. The characteristic bands of MoO_3 show absorbance bands around 999-995, 900-877, 561-554 cm^{-1} [30]. Furthermore, the additional characteristic peaks for Co_3O_4 show around 667, 626, and 580 cm^{-1} [31,32]. This FT-IR analysis provides additional data implementation for as-prepared catalysts and supports the characterization of the XRD diffractogram, which shows the successful process of preparation catalysts.

Scanning Electron Microscopy (SEM) characterization provides information on the catalyst morphology. Figure 4 informs the morphology of all as-prepared catalysts showing the coffin-like or hexagonal crystal geometry [33]. Specific to the Figure 3 (c)-(f), the Co or Mo oxides anchoring to the catalyst's surface contributes to changing the surface of the ZSM-5 catalysts to become slightly rougher.

The elemental composition of the catalyst is analyzed by XRF and EDS methods. The XRF data reveals the element composition in a
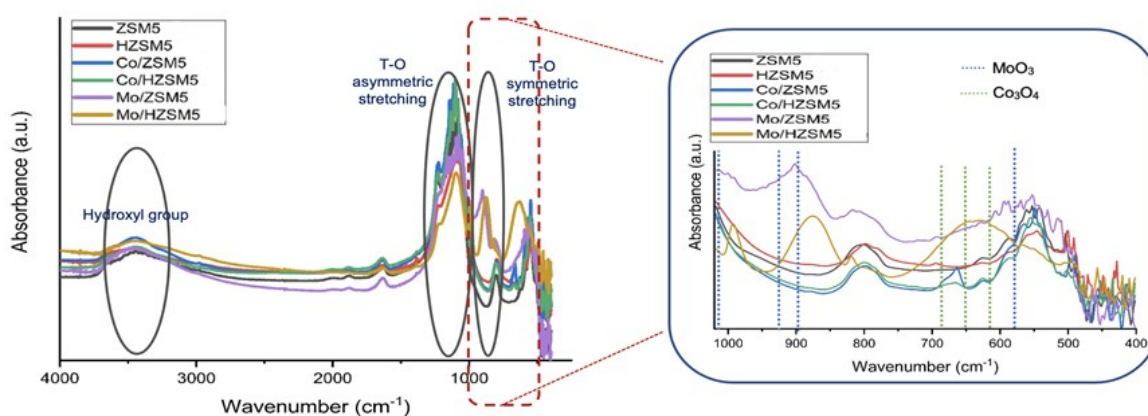

Figure 3. FT-IR spectra of as-prepared catalysts

bulky state, while the EDS data show the composition of the elements on the surface. The summary of the Si/Al ratio and the loaded metal of the catalysts are shown in Table 1. Generally, based on XRF data, there was no significant change in the Si/Al ratio of the catalyst after the preparation of HZSM-5 and the metal oxide impregnation process. In addition, the EDS data showed that the %wt of Na content was significantly decreased in HZSM-5, indicating an effective cation exchange process. Furthermore, the %wt loading of the Co-oxide and Mo-oxide is close to the expected amount of metal oxide. As for metal oxides that are not incorporated into the catalyst, it could be caused by the aggregation of metal oxide groups on the outside of the catalyst.

Furthermore, the porosity and textural properties of the catalyst were analyzed using the BET and BJH methods. The adsorption-desorption isotherm graphs (Figure 5) show that as-prepared catalysts have a type IV isotherm curve, which indicates monolayer adsorption at low pressure and multilayer adsorption in high pressure, and with the existence of hysteresis loop that indicates the hierarchical porosity [33-35]. The adsorption and desorption isotherm curves show small hysteresis, that could be due to the existence of impurities from the natural precursors which influenced the formation of pores in ZSM-5. Furthermore, from discussion in XRD data, it can also be seen that there is a quartz phase that might cause pore-blocking within the ZSM-5 framework.

Tabel 1. Summary Si/Al and metal loading (%wt) in catalysts by XRF and EDS method

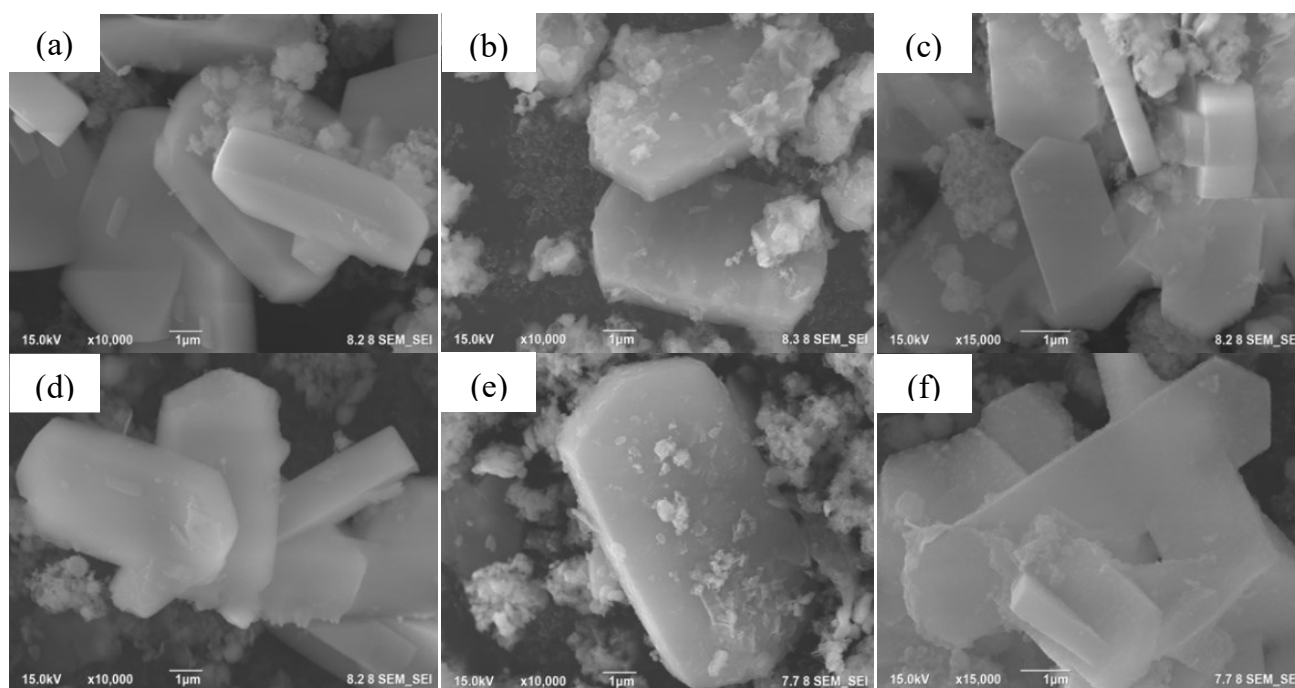| Catalyst	XRF			EDS			
	Mo	Co	Si/Al Ratio	Na	Mo	Co	Si/Al Ratio
ZSM-5	-	-	12.11	1.20	-	-	14.12
HZSM-5	-	-	13.20	0.50	-	-	14.65
CoO_x/ZSM-5	-	8.30	11.44	-	-	7.00	12.04
MoO_x/ZSM-5	7.94	-	11.30	-	9.60	-	11.32
CoO_x/HZSM-5	-	7.36	12.12	-	-	7.80	10.11
MoO_x/HZSM-5	8.19	-	11.19	-	10.30	-	12.00

Figure 4. SEM images for (a) ZSM-5, (b) MoO_x/ZSM-5, (c) CoO_x/ZSM-5, (d) HZSM-5, (e) MoO_x/HZSM-5, (f) CoO_x/HZSM-5 catalyst

The process of cation exchange showed not to significantly change the structural porosity of the catalyst and the textural properties tended to be preserved. Meanwhile, the incorporation of metal oxides in catalysts shows that all the catalysts experienced a reduction in BET surface area except the CoO$_x$/HZSM-5. This decrease was mainly due to solid metal species at the pores and/or the external surface of zeolites [21]. Meanwhile, the MoO$_x$/ZSM-5 experiences a significant decrease in BET surface area and pore volume. This condition is because of the agglomeration of Mo oxide in the pore.

In contrast, the increase of surface area in CoO$_x$/HZSM-5 due to the aggregation of Co-oxides on the external zeolite surface, which leads to the creation of more volume and pore. This phenomenon was also observed by Krisnandi *et al.* when preparing iron oxide modified NaY Zeolite [36]. Moreover, the *t*-Plot analysis

showed the metal oxides reside in both micropores and mesopores catalysts. The textural properties of the catalysts are summarized in Table 2.

Data from Table 2 show that Mo impregnated HZSM-5 led to the pore opening in the mesopore site of catalysts which made a larger size in the distribution pores. Seen also in XRF data of MoO$_x$/HZSM-5, that experienced a decrease of Si/Al ratio from 13.20 to 11.19 compared to the HZSM-5 was assumed due to desilication. It was also reported by Kosinov *et al.* that most of the initially aggregated Mo-oxide at the external surface are dispersed into the pore upon calcination, resulting in the reaction of mobile MoO$_3$ species with framework Al, aluminum molybdate formation, and produced the amorphous SiO$_2$ [37].

The acidity of ZSM-5 and modified ZSM-5 catalysts was determined by NH$_3$-TPD as de-

Tabel 2. Summary of textural properties catalysts based on N$_2$-sorption analysis

Catalyst	Surface Area (m²/g)			Volume @STP (cc/g)			[g]Pore Distribution (nm)	
	[a]BET	[b]Micro	[c]Meso	[d]Total	[e]Micro	[f]Meso	Micro	Meso
ZSM-5	159	75	84	0.11	0.04	0.07	1.93	3.12
HZSM-5	149	70	79	0.10	0.04	0.07	1.94	2.73
CoO$_x$/ZSM-5	152	72	80	0.11	0.04	0.07	1.93	2.16
MoO$_x$/ZSM-5	58	25	34	0.04	0.01	0.03	1.94	2.16
CoO$_x$/HZSM-5	193	84	110	0.13	0.04	0.08	1.93	2.16
MoO$_x$/HZSM-5	139	54	85	0.14	0.03	0.11	1.94	9.28

[a]BET surface area; [b]Micropore surface area evaluated by *t*-plot method; [a]BET surface area, [b]Micropore surface area evaluated by *t*-plot method; [c]Mesopore surface area calculated using S_{BET}-S_{micro}, [d]Total pore volume at P/P0 ~ 0.99; [c]Mesopore surface area calculated using S_{BET}-S_{micro}, [d]Total pore volume at P/P0 ~ 0.99; [e]Micropore volume calculated by *t*-plot method; [f]Mesopore volume calculated using V_{Total}-V_{micro}; [e]Micropore volume calculated by *t*-plot method; [f]Mesopore volume calculated using V_{Total}-V_{micro}; [g]Pore distribution based on BJH analysis.
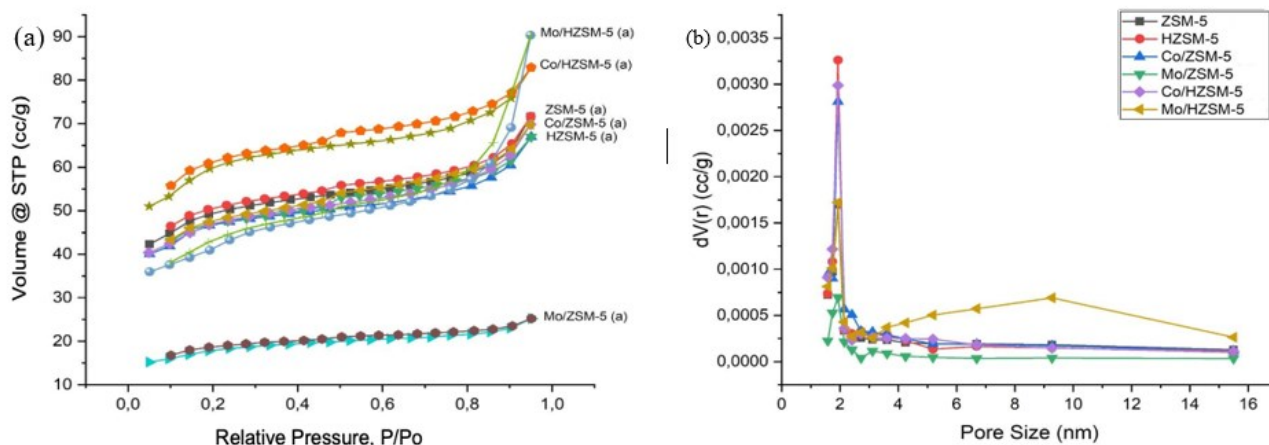

Figure 5. (a) Isotherm of adsorption-desorption curves and (b) pore size distribution of as-prepared catalysts

picted in Figure 6. The temperature-programmed desorption of a basic molecule, such as ammonia (NH_3-TPD), is one of the most commonly used methods for measuring the surface acidity of porous materials such as zeolites [21,38-39]. With the NH_3-TPD analysis, the acid site distribution in catalysts could be estimated. Generally, the acidity distribution can be divided into three regions by Gaussian function as a weak acid, moderate acid, and strong acid site [21,46]. Specific to the ZSM-5 and HZSM-5 acidity profile, the peaks of acid distribution usually appear in two temperature regions [47] or three temperature regions [21,46].

In Figure 6, each curve was divided into three peaks as Gaussian function; the peaks centered ca. 100-250 °C, 250-600 °C, and 600-800 °C pointing to the desorption of NH_3 in weak acid, medium acid, and strong acid positions [21]. The low Si/Al ratio (Si/Al ratio = 12) in as-prepared catalysts caused the NH_3 desorption in medium and strong acid sites was found in high temperature regions. It was also reported by Lonyi *et al*. that the NH_3-TPD curve of HZSM-5 with Si/Al ratio = 15 have a high temperature region around 550-700 °C [39]. Table 3 shows the summary of detailed catalysts acidity information of as-prepared catalysts.

Furthermore, Mo incorporated ZSM-5 and HZSM-5 has interestingly changed the acid site property from the strong acid to weak acid, with the % weak acid content being 48% and 42%, respectively. Meanwhile, the CoO_x/ZSM-5 has strong acid as the dominant acid sites, while CoO_x/HZSM-5 is predominated with medium acid sites.

The change in the acidity of the catalyst is associated with the closure of the acid sites on the surface and the reaction between metal species and the acid site on the outer surface or in the channels [21,38,40]. In addition, the data shows the impregnation lead reaction between metal species and protonic acid and would have converted the strong acid into a medium or weak acid.

3.2. Catalytic Activity

The % conversion of the DPE substrate was displayed in Figure 7, showing that the % conversion of DPE was about 89-91% conversion for the uncatalyzed reaction, and 96-100% conversion when catalysts were added, with the highest using the MoO_x/HZSM-5 catalyst at 200 °C was 100% conversion.

Figure 8 reveals the % yield of the desired compounds of this reaction, phenol and vanillin. The Figure 7(a) shows without a catalyst, the % yields of phenol fall in the range of 10% - 18%, the highest was 17.65% at 200 °C, while in the presence of catalysts, the % yield of phenol was increased, with the highest yield of
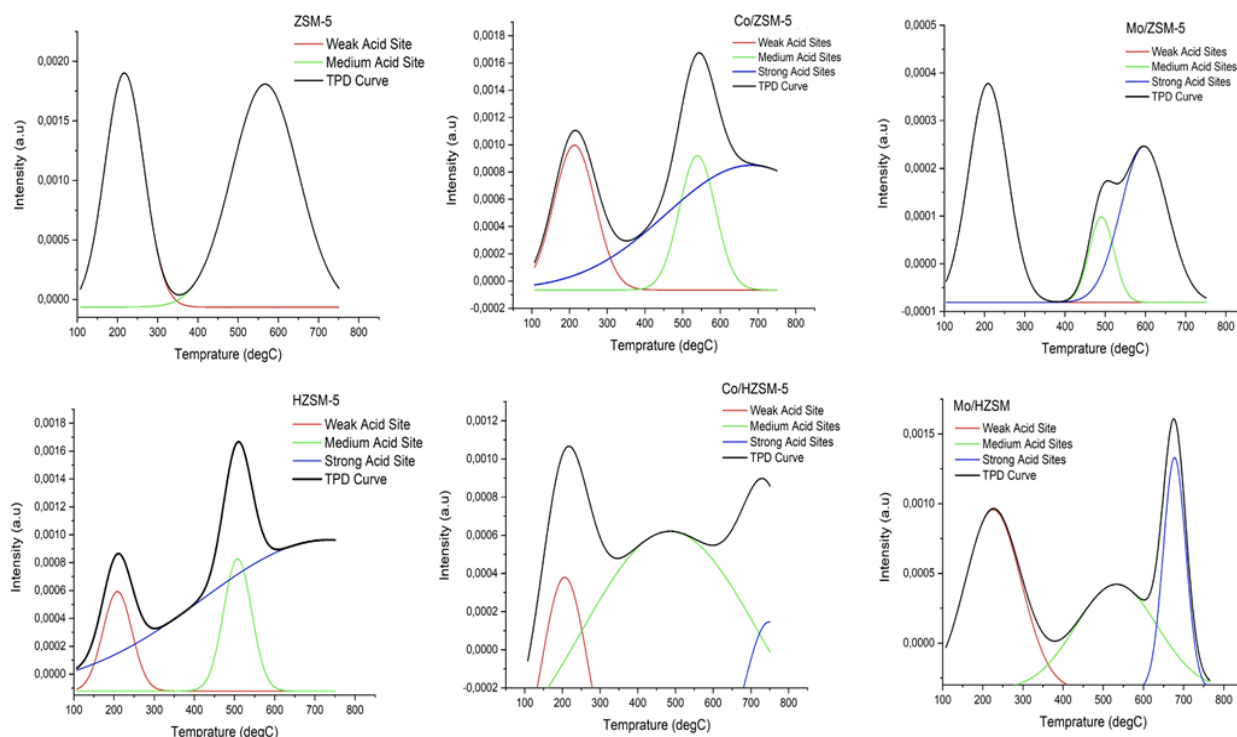

Figure 6. NH_3-TPD curves from as-prepared catalysts

31.96 % was achieved using MoO$_x$/HZSM-5 catalyst at 250 °C. On the other hand, for vanillin, as shown in Figure 8(b), the highest yield was 7.63% over MoO$_x$/HZSM-5 catalyst at a temperature of 200 °C.

3.3. Correlation of Physicochemical Properties of Catalysts and the Catalytic Activity

The reaction of DPE molecules as organic molecules is influenced by temperature, so as expected the % conversion of DPE at the reaction temperature (150-250 °C) was high, nearly 100%. It has also been reported that the breaking of C−O−C and aryl ether bonds can occur in the temperature range of 150-300 °C without using a catalyst [41]. Yao *et al.* reported that over numerous heterogenous catalysts the DPE conversion above 70% in 120 °C [42], furthermore, Zhao *et al.* reported over Pd/C and HZSM-5 in aqueous solution, DPE are converted 100% at 200 °C [43]. However, it becomes

important to use a catalyst in the reaction to increase the selectivity of desired products, such as vanillin and phenol. In addition, this study showed that phenol and vanillin are the major products from DPE substrate over the as-prepared catalysts. The other possible products are benzene, cyclohexane, cyclohexanol and cyclohexanone, as reported in [44,45]. Thus, further product analysis using other standard compounds or with Liquid Chromatography-Mass Spectrometry (LC-MS) is suggested to be carried out if necessary. According to the catalytic activity and the physicochemical properties, the character of the catalyst that has a significant influence on the production of phenol and vanillin is the composition of the catalyst acidity and the textural/porosity properties.

As observed in this study, where ZSM-5 has two desorption peaks and HZSM-5 has three desorption peaks in NH$_3$-TPD curve as depicted in Figure 6. Furthermore, Engtrakul *et al.*

Table 3. Acidity profile by NH$_3$-TPD measurement of as-prepared catalysts

Catalyst	Acid Amount (mmol/g)	*Acid Site Content (%)			Peak Position (ºC)		
		Weak	Medium	Strong	Weak	Medium	Strong
ZSM-5	0.2870	38	62	0	207	568	-
HZSM-5	0.2199	6	8	85	221	510	703
CoO$_x$/ZSM-5	0.1803	19	15	66	220	557	726
MoO$_x$/ZSM-5	0.0532	48	12	41	207	502	635
CoO$_x$/HZSM-5	0.2595	15	72	13	214	475	732
MoO$_x$/HZSM-5	0.1512	42	36	22	224	526	676

*Acid Content determined by NH$_3$-TPD profile deconvolution with Gaussian peaks (R^2 > 0.95)

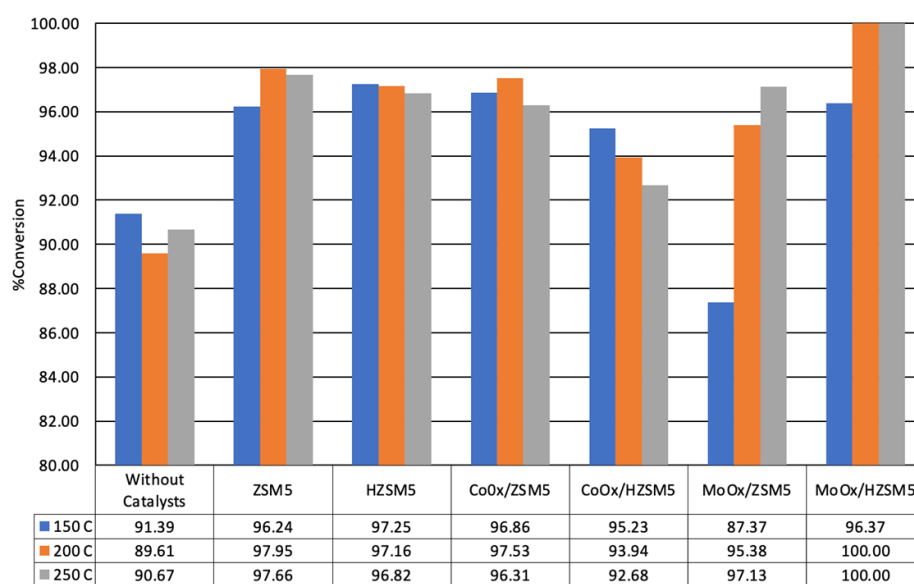|	Without Catalysts	ZSM5	HZSM5	CoOx/ZSM5	CoOx/HZSM5	MoOx/ZSM5	MoOx/HZSM5
150 C	91.39	96.24	97.25	96.86	95.23	87.37	96.37
200 C	89.61	97.95	97.16	97.53	93.94	95.38	100.00
250 C	90.67	97.66	96.82	96.31	92.68	97.13	100.00

Figure 7. DPE conversion over as-prepared catalysts; reaction condition: P N$_2$ = 2 atm DPE : catalyst ratio = 0.25 g : 0.125 g, solvent used (ethanol:H$_2$O) = 1:1 in total volume was 25 mL

reported that the temperature peaks are influenced by the Si/Al ratio of the catalysts, which the lower Si/Al can shift the peaks to higher temperature region [39,48].

In addition, the incorporation of metal oxides in zeolite has been reported can change the catalysts' acidity, such as new peaks appearing at high-temperature regions [47] and changing the dominant composition of the acid sites [21,28,49,50]. Specific to incorporated with molybdenum oxide, the low temperature desorption peak experienced an increase [28,49]. Meanwhile, the incorporation with cobalt oxide

tends to increase desorption peak at higher temperature region [50]. This phenomenon is similar to what was found in this study, that incorporating molybdenum oxide can increase acidity in the low-temperature region. In contrast with the cobalt oxides can increase acidity in relatively high temperature region.

Specific to the expected mild conditions in this study, where the reaction temperature is low, ranging from 150-250 °C, it is seen that the catalyst with the high weak acid content can facilitate the reaction optimally. The modified Mo catalyst with the weak acid content
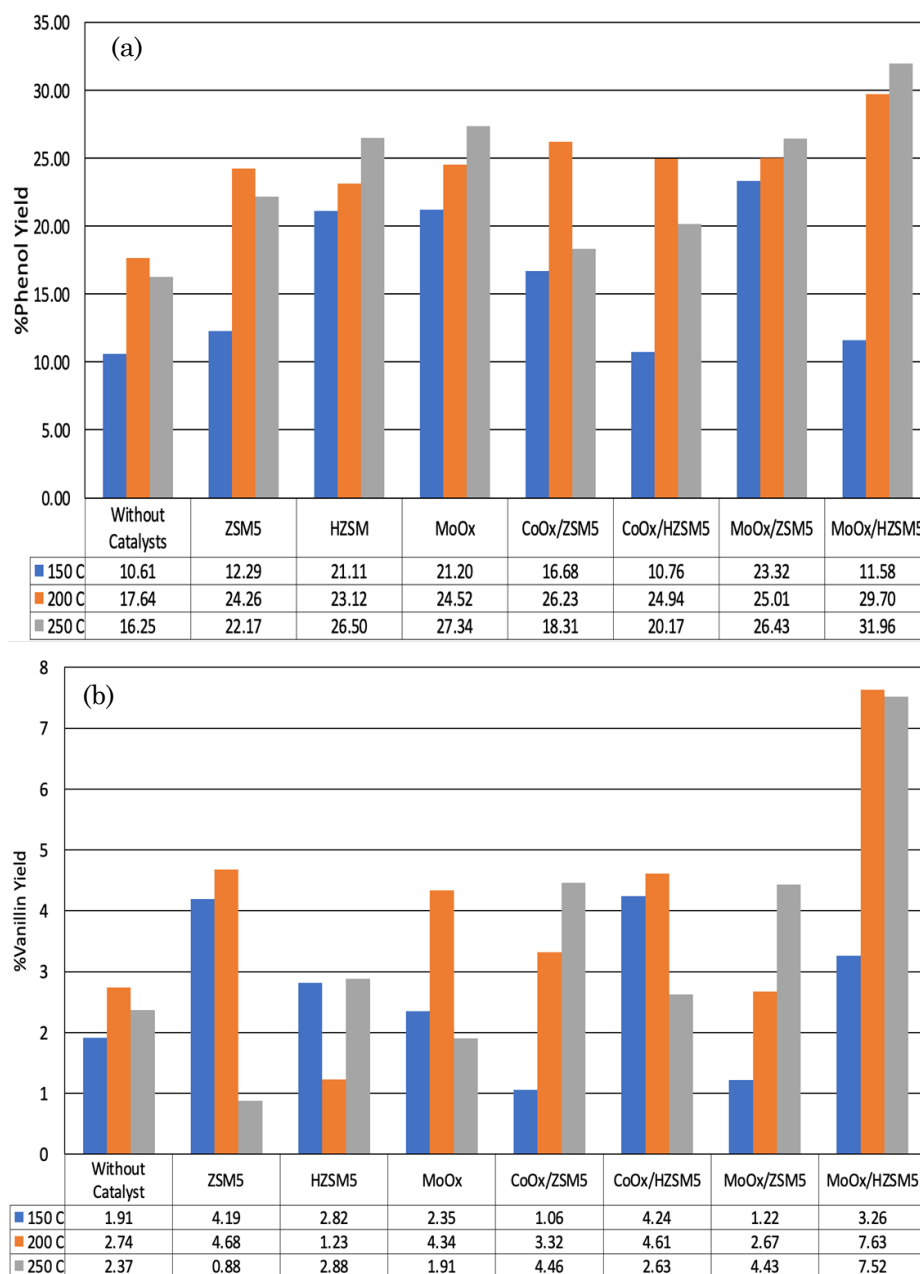

	Without Catalysts	ZSM5	HZSM	MoOx	CoOx/ZSM5	CoOx/HZSM5	MoOx/ZSM5	MoOx/HZSM5
■ 150 C	10.61	12.29	21.11	21.20	16.68	10.76	23.32	11.58
■ 200 C	17.64	24.26	23.12	24.52	26.23	24.94	25.01	29.70
■ 250 C	16.25	22.17	26.50	27.34	18.31	20.17	26.43	31.96

	Without Catalyst	ZSM5	HZSM5	MoOx	CoOx/ZSM5	CoOx/HZSM5	MoOx/ZSM5	MoOx/HZSM5
■ 150 C	1.91	4.19	2.82	2.35	1.06	4.24	1.22	3.26
■ 200 C	2.74	4.68	1.23	4.34	3.32	4.61	2.67	7.63
■ 250 C	2.37	0.88	2.88	1.91	4.46	2.63	4.43	7.52

Figure 8. Percentage of yield of (a) phenol and (b) vanillin from DPE substrate over as-prepared Catalysts, reaction condition: P N$_2$ = 2 atm DPE : catalyst ratio = 0.25 g : 0.125 g, solvent used (ethanol:H$_2$O) = 1:1 in total volume was 25 mL

above 40% shows the highest production of phenol and vanillin at a reaction temperature of 200-250 °C. It was also reported by Jiang *et al.* that cleavage of diphenyl ether C−O bond optimally facilitated over weakly acidic catalyst in 220 ºC [51].

Moreover, in more detail on the NH$_3$-TPD analysis, apart from the number of catalyst acid sites, the ability of the modified Mo oxide catalyst in adsorbing and desorbing substrate molecules (base species) from the surface greatly supports the performance of heterogeneous catalysts, where the ability of the active site of the catalyst to adsorb-desorb substrates and products is one of the important factors. Furthermore, the Navajas *et al.* also reported that the Molybdenum oxides have interesting activity regarding the active sites as the Lewis acid and the Brönsted acid in the conversion of vegetable oil [52]. Considering the Lewis acidity, the molybdenum species could provide the orbital *d* and can form the reactive transition state with the substrate and lead the lower energy pathway in the reaction. It showed that increasing acidity in the low-temperature region could support the conversion reaction in mild conditions due to the ability to give the hydrogen from the surface to react with the substrate. Furthermore, supported by Ben *et al.* the existence of hydrogen as the Brönsted acid site in catalyst can facilitate some reactions in lignin conversions, such as hydrodeoxygenation (the carbocation formed by dehydration), followed by cleavage ether bond, decarboxylation, or cleavage of the C−C bond [53].

In addition to the acidity of the catalyst, it is also seen that the mesopore size influences the tendency for the formation of phenol and vanillin products in the catalyst. The presence of mesopore in the catalyst increases the catalytic effectiveness, where the larger the size of the mesopore, the higher the yield of the desired product [54,55]. In this study, the mesopore size above 9 nm gives the highest production of phenol and vanillin.

Interestingly, although it has a dominance of a weak acid, if the catalyst does not have a large mesopore size, then the production of phenol and vanillin is not optimal. It can be seen in catalytic activity, where MoO$_x$/ZSM-5 with 48% weak acid but only 2.16 nm mesopore size resulted in the production of phenol and vanillin under the MoO$_x$/HZSM-5 catalyst, which had 42% weak acid content with 9.28 nm mesopore size. The size of the mesopore greatly affects the ability of the substrate and product to diffuse into the pore. Kantarelis *et al.* also reported that the coke formation formed during the reaction and led to the blockage in the pore [7]. Meanwhile, with the larger pore size (by introducing mesoporosity), this drawback can be overcome. Therefore, this work revealed that the yield of phenol and vanillin products in the catalytic reaction of DPE as a lignin model compound was correlated with the content of weak acid on the catalyst and, at the same time, the mesopore size in the catalyst. Therefore, this study can recommend that ZSM-5 synthesized with higher weak acid content and large mesoporosity can facilitate the conversion of lignin at the mild condition with low temperatures, ranging from 200-250 °C.

3.4 Proposed Reaction Mechanism

Based on Figure 9 and considering the resulting yield, the DPE conversion mechanism is thought to be initiated by the formation of phenol followed by vanillin. This reaction is fa-

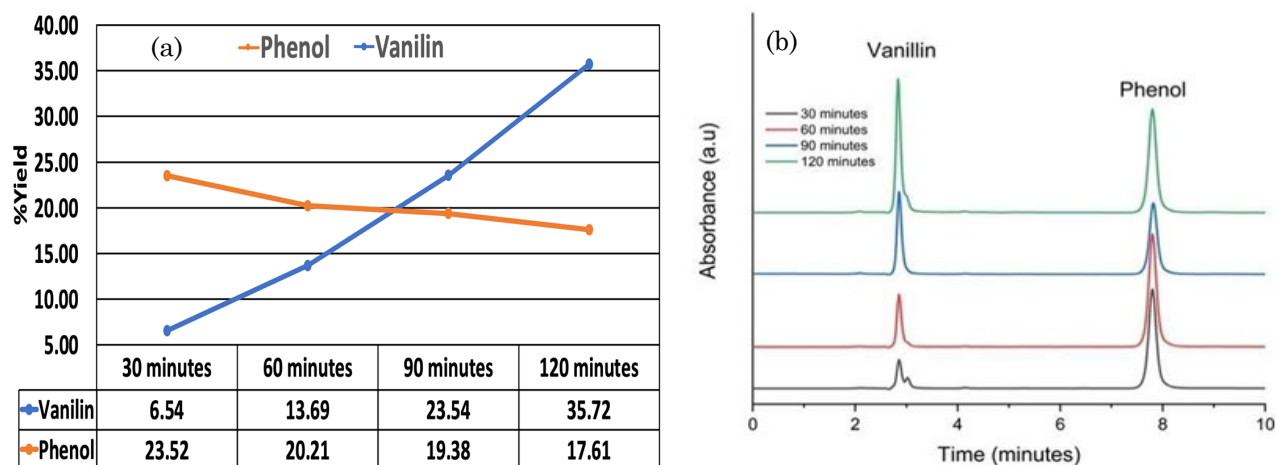|	30 minutes	60 minutes	90 minutes	120 minutes
Vanilin	6.54	13.69	23.54	35.72
Phenol	23.52	20.21	19.38	17.61

Figure 9. (a) Percentage of yield of phenol and vanillin, and (b) Chromatogram of product from DPE substrate over Mo/HZSM-5 catalyst in various time reaction

cilitated by hydrogen on the catalyst surface and breaks the ether bond [44]. It is similar to the observation by Yao *et al.* that phenol is the major product of conversion DPE in 140 °C in one hour reaction by the hydrodeoxygenation pathway [39]. This reaction begins with the adsorption of the substrate molecule on its oxygen (base substituent) on the acidic side of catalyst, probably the Mo oxide on the surface of the catalyst and is followed by a chemical reaction on the surface due to the presence of hydrogen in the catalyst surface. It has been reported the Mo-based catalysts selectively break C−O bond, meanwhile preserve the aromatic ring [53]. Moreover, Mo oxide species is generally considered as the originate of high hydrodeoxygenation activity over Mo-based catalysts [54]. The reaction continues to produce vanillin, the presence of supported Mo oxide facilitates the reaction of the oxidation from ethanol as a solvent to an aldehyde substituent, supported by report in [11,55]. The presence of Brönsted acid in the catalyst surface leads to the formation of a carbocation and termination of the C−C bond to produce methoxy, similar to the report in [50]. The description of these stages can be seen in Figure 10.

4. Conclusions

In this study, the as-synthesized and modified ZSM-5 catalysts from alternative precursors i.e Indonesian zeolite and Kaolin showed physicochemical properties that have met the criteria for good heterogeneous catalyst in DPE lignin model compound conversion to phenol and vanillin. The relationship between the physicochemical properties of the catalysts has been investigated. To conclude, MoO_x/HZSM-5 catalyst, which has dominance of weak acid composition above 40% and with the mesopore size of 9 nm, showed the highest % yields of phenol and vanillin, at reaction temperature of 200-250 °C in 30 minutes reaction.
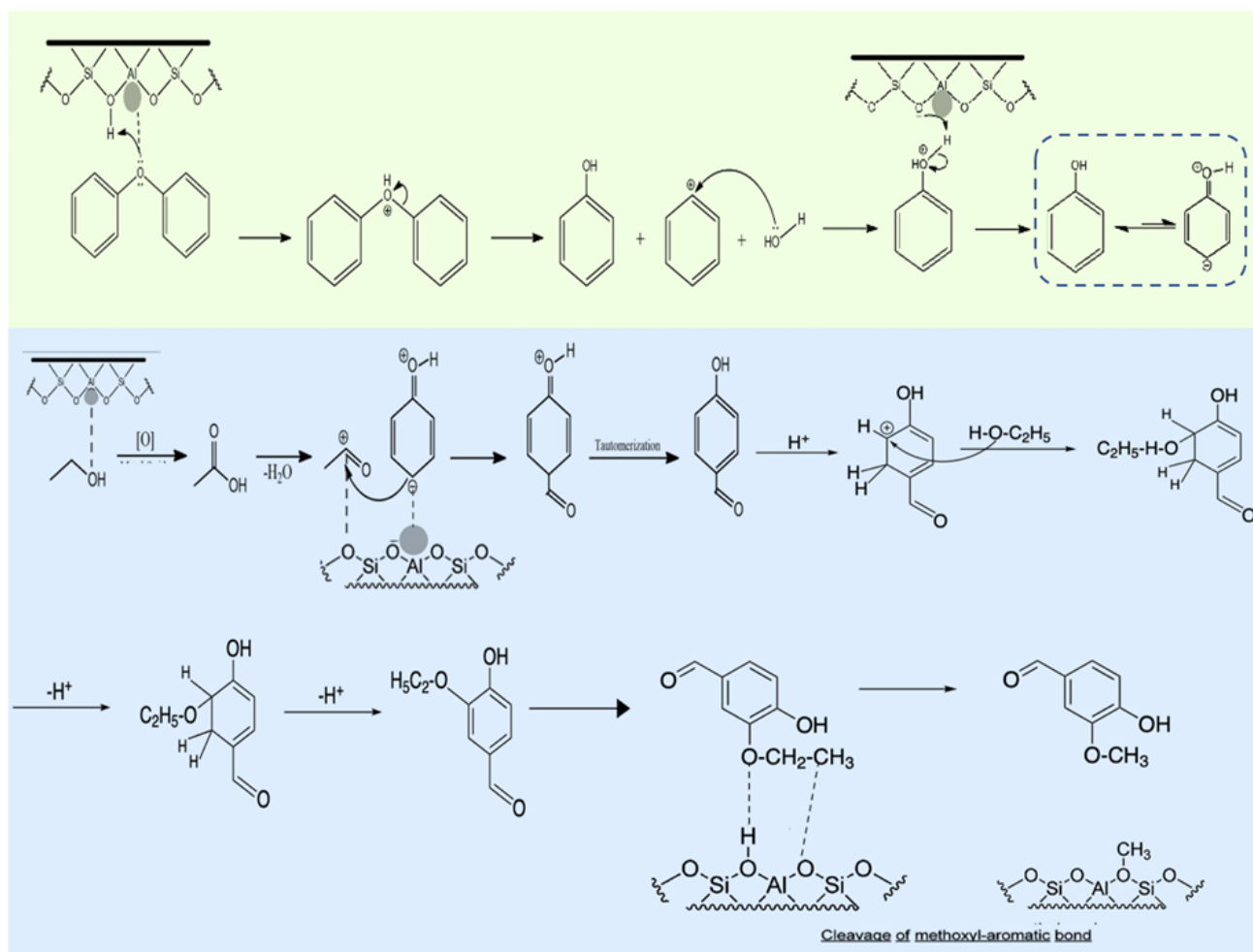

Figure 10. Proposed mechanism to produce vanillin from DPE with phenolic compound as the intermediate over MoO_x/HZSM-5 catalyst

Acknowledgements

References

[1] Li, C., Zhao, X., Wang, A., Huber, G.W., Zhang, T. (2015). Catalytic Transformation of Lignin for the Production of Chemicals and Fuels. *Chem. Rev.*, 115 (21), 11559–11624. DOI: 10.1021/acs.chemrev.5b00155.

[2] Guadix-Montero, S., Sankar, M. (2018). Review on Catalytic Cleavage of C–C Inter-unit Linkages in Lignin Model Compounds: Towards Lignin Depolymerisation. *Top. Catal.*, 61 (3–4), 183–198, DOI: 10.1007/s11244-018-0909-2.

[3] Liu, C., Wu, S., Zhang, H., Xiao,R. (2019). Catalytic oxidation of lignin to valuable biomass-based platform chemicals: A review. *Fuel Process. Technol.*, 191, 181–201, DOI: 10.1016/j.fuproc.2019.04.007

[4] Mauriello, F.F., Paone, E., Pietropaolo, R., Balu, A.M., Luque, R. (2018). Catalytic transfer hydrogenolysis of lignin derived aromatic ethers promoted by bimetallic Pd / Ni systems. *ACS Sustainable Chem. Eng.* 6 (7), 9269-9276, DOI: 10.1021/acssuschemeng.8b01593.

[5] Hu, C., Zhang, H., Wu, S., Xiao, R. (2020). Molecular shape selectivity of HZSM-5 in catalytic conversion of biomass pyrolysis vapors: The effective pore size. *Energy Conversion and Management*, 210, 112678. DOI: 10.1016/j.enconman.2020.112678.

[6] Deepa, A.K., Dhepe, P.L. (2014). Solid acid catalyzed depolymerization of lignin into value added aromatic monomers. *RSC Adv.*, 4 (25), 12625–12629, DOI: 10.1039/c3ra47818a.

[7] Kantarelis, E., Javed, R., Stefanidis, S., Psarras, A., Iliopoulou, E., Lappas, A. (2019). Engineering the Catalytic Properties of HZSM5 by Cobalt Modification and Post-synthetic Hierarchical Porosity Development. *Top Catal.*, 62 (7–11), 773–785, DOI: 10.1007/s11244-019-01179-w.

[8] Xie, W., Liang, J., Morgan, H.M., Zhang, X., Wang, K., Mao, H., Bu, Q. (2018). Ex-situ catalytic microwave pyrolysis of lignin over Co/ZSM-5 to upgrade bio-oil. *Journal of Analytical and Applied Pyrolysis*, 132, 163-170. DOI: 10.1016/j.jaap.2018.03.003.

[9] Ma, Z., Custodis, V., Van Bokhoven, J.A. (2014). Selective deoxygenation of lignin during catalytic fast pyrolysis. *Catal. Sci. Technol.*, 4 (3), 766–772. DOI: 10.1039/c3cy00704a.

[10] Sun, L., Wang, Z., Chen, L., Yang, S., Xie, X., Gao, M., Zhao, B., Si, H., Li, J., Hua, D. (2020). Catalytic Fast Pyrolysis of Biomass into Aromatic Hydrocarbons over Mo-Modified ZSM-5 Catalysts. *Catalysts*, 10(9), 1051. DOI: 10.3390/catal10091051.

[11] Zhang, L., Wang, Y., Zhang, L., Chi, Z., Yang, Y., Zhang, Z., Zhang, B., Lin, J., Wan, S. (2020). Hydrogenolysis of Aryl Ether Bond over Heterogeneous Cobalt-Based Catalyst. I*ndustrial & Engineering Chemistry Research,* 59 (39), 17357-17364. DOI: 10.1021/acs.iecr.0c01374

[12] Prasomsri, T., Nimmanwudipong, T., Román-Leshkov, Y. (2013). Effective hydrodeoxygenation of biomass-derived oxygenates into unsaturated hydrocarbons by MoO_3 using low H_2 pressures. *Energy & Environmental Science,* 6(6), 1732-1738. DOI: 10.1039/c3ee24360e

[13] Jing, Y., Dong, L., Guo, Y., Liu, X., Wang, Y. (2019). Chemicals from lignin: a review of the catalytic conversion involving hydrogen. *ChemSusChem,* 13 (17), 4181-4198. DOI: 10.1002/cssc.201903174

[14] Asghari, A., Khorrami, M.K., Kazemi, S.H. (2019). Hierarchical H-ZSM5 zeolites based on natural kaolinite as a high-performance catalyst for methanol to aromatic hydrocarbons conversion. *Scientific Reports*, 9(1), 17526. DOI: 10.1038/s41598-019-54089-y.

[15] Krisnandi, Y.K., Saragi, I.R., Sihombing, R., Ekananda, R., Sari, I.P., Griffith, B.E., Hanna, J.V. (2019). Synthesis and Characterization of Crystalline NaY-Zeolite from Belitung Kaolin as Catalyst for n-Hexadecane Cracking. *Crystals,* 9 (8), 404-417. DOI: 10.3390/cryst9080404.

[16] Yue, Y., Kang, Y., Bai, Y., Gu, L., Liu, H., Bao, J., Wang, T., Yuan, P., Zhu, H., Bai, Z., Bao, X. (2018). Seed-assisted, template-free synthesis of ZSM-5 zeolite from natural aluminosilicate minerals. *Applied Clay Science,* 158, 177–185. DOI: 10.1016/j.clay.2018.03.025

[17] Pratama, A.P., Krisnandi, Y.K., Abdullah, I. (2020). Catalytic depolymerization of lignin from wood waste biomass over natural sourced ZSM-5 catalysts Catalytic depolymerization of lignin from wood waste biomass over natural sourced ZSM-5 catalysts. In *IOP Conference Series: Materials Science and Engineering* pp. 1–8. 4th International Symposium on Current Progress in Functional Materials 2019. DOI: 10.1088/1757-899X/902/1/012051

[18] Rohayati, R., Krisnandi, Y.K., Sihombing, R. (2017). Synthesis of ZSM − 5 zeolite using Bayat natural zeolite as silica and alumina source Synthesis of ZSM − 5 Zeolite Using Bayat Natural Zeolite as Silica and Alumina Source. In *AIP Conference Proceedings.* International symposium on current progress in mathematics and sciences (ISCPMS 2016) 1862, 030094. DOI: 10.1063/1.4991198.

[19] Wang, L., Zhang, Z., Yin, C., Shan, Z., Xiao, F. (2010) Microporous and Mesoporous Materials Hierarchical mesoporous zeolites with controllable mesoporosity templated from cationic polymers, *Microporous and Mesoporous Materials*, 131 (1–3), 58–67, DOI: 10.1016/j.micromeso.2009.12.001.

[20] Wang, X., Du, B., Pu, L., Guo, Y., Li, H., Zhou, J. (2018). Effect of particle size of HZSM-5 zeolite on the catalytic depolymerization of organosolv lignin to phenols, *J. Anal. Appl. Pyrolysis*, 129, 13–20, DOI: 10.1016/j.jaap.2017.12.011.

[21] Che, Q., Yang, M., Wang, X., Yang, Q., Rose Williams, L., Yang, H., Zou, J., Zeng, K., Zhu, Y., Chen, Y., Chen, H. (2019). Influence of physicochemical properties of metal modified ZSM-5 catalyst on benzene, toluene and xylene production from biomass catalytic pyrolysis. *Bioresource Technology*, 278, 248-254. DOI: 10.1016/j.biortech.2019.01.081.

[22] Krisnandi, Y.K., Putra, B.A.P., Bahtiar, M., Zahara, Z., Abdullah, I., Howe, R.F. (2015). Partial Oxidation of Methane to Methanol over Heterogeneous Catalyst Co/ZSM-5. *Procedia Chemistry*, 14, 508–515. DOI: 10.1016/j.proche.2015.03.068.

[23] Liu, B., France, L., Wu, C., Jiang, Z., Kuznetsov, V.L., Al-Megren, H.A., Al-Kinany, M., Aldrees, S.A., Xiao, T., Edwards, P.P. (2015). Methanol-to-hydrocarbons conversion over MoO₃/H-ZSM-5 catalysts prepared via lower temperature calcination: a route to tailor the distribution and evolution of promoter Mo species, and their corresponding catalytic properties, *Chem. Sci.*, 6 (9), 5152–5163, DOI: 10.1039/c5sc01825k.

[24] Caldeira, V.P.S., Santos, A.G.D., Pergher, S.B.C., Costa, M.J.F., Araujo, A.S. (2016), Use of a low-cost template-free zsm-5 for atmospheric petroleum residue pyrolysis, *Quim. Nova*, 39 (3), 292–297, DOI: 10.5935/0100-4042.20160019.

[25] Colella, C., Wise, W.S. (2014). The IZA Handbook of Natural Zeolites: A tool of knowledge on the most important family of porous minerals. *Microporous Mesoporous Mater.*, 189, 4–10, DOI: 10.1016/j.micromeso.2013.08.028.

[26] Omar, B.M., Bita, M., Louafi, I., Djouadi, A. (2018), Esterification process catalyzed by ZSM-5 zeolite synthesized via modified hydrothermal method, *Methods X*, 5, 277–282, DOI: 10.1016/j.mex.2018.03.004.

[27] Sun, J., Wang, H., Li, Y., Zhao, M. (2021). Porous Co₃O₄ column as a high-performance Lithium anode material. *J. Porous Mater.*, 28 (3), 889–894, DOI: 10.1007/s10934-021-01041-z.

[28] Li, Z., Yang, J., Zhou, Y., Cui, J., Ma, Y., Geng, C., Kang, Y., Liu, J., Yang, C. (2020). Influence of different preparation methods on the activity of Ce and Mo co-doped ZSM-5 catalysts for the selective catalytic reduction of NOx by NH₃, *Environ. Sci. Pollut. Res.*, 27 (32), 40495–40503, DOI: 10.1007/s11356-020-10052-3.

[29] Zhang, Y., Zhu, K., Duan, X., Li, P., Zhou, X., Yuan, W. (2014). Synthesis of hierarchical ZSM-5 zeolite using CTAB interacting with carboxyl-ended organosilane as a mesotemplate. *RSC Adv.*, 4 (28), 14471–14474, DOI: 10.1039/c3ra46646a.

[30] Wang, L., Xu, Y., Tan, X., Tapas, S., Zhang, J. (2017). Aim and shoot: Molecule-imprinting polymer coated MoO₃ for selective SERS detection and photocatalytic destruction of low-level organic contaminants. *RSC Adv.*, vol. 7, no. 58, pp. 36201−36207, DOI: 10.1039/c7ra05547a.

[31] Anuradha, C.T., Raji, P. (2020). Facile synthesis and characterization of Co₃O₄ nanoparticles for high-performance supercapacitors using Camellia sinensis. *Appl. Phys. A Mater. Sci. Process.*, 126 (3), DOI: 10.1007/s00339-020-3352-8.

[32] Zhou, X.J., Shi, P.H., Qin, Y.F., Fan, J.C., Min, Y.L., Yao, W.F. (2016). Synthesis of Co₃O₄/graphene composite catalysts through CTAB-assisted method for orange II degradation by activation of peroxymonosulfate. *J. Mater. Sci. Mater. Electron.*, 27 (1), 1020–1030, DOI: 10.1007/s10854-015-3847-9.

[33] Krisnandi, Y.K., Nurani, D.A., Reza, M., Samodro, B.A., Suwardiyanto, S., Susianto, N., Putrananda, A.T., Saragi, I.R., Umar, A., Choi, S.-M., Howe, R.F. (2019). Partial Oxidation of Methane to Methanol on Cobalt Oxide-Modified Hierarchical ZSM-5. *Biogas - Recent Advances and Integrated Approaches* May, Intech Open Publisher. DOI: 10.5772/intechopen.86133.

[34] Cui, H.J., Shi, J.W., Yuan, B., Fu, M.L. (2013). Synthesis of porous magnetic ferrite nanowires containing Mn and their application in water treatment. *J. Mater. Chem. A*, 1 (19), 5902–5907, DOI: 10.1039/c3ta01692g.

[35] Goyal, A., Bansal, S., Samuel, P., Kumar, V. , Singhal, S. (2014). CoMn$_{0.2}$Fe$_{1.8}$O$_4$ ferrite nanoparticles engineered by sol-gel technology: An expert and versatile catalyst for the reduction of nitroaromatic compounds. *J. Mater. Chem. A*, 2 (44), 18848–18860, DOI: 10.1039/c4ta03900a.

[36] Krisnandi, Y.K., Nurani, D.A., Alfian, D.V., Sofyani, U., Faisal, M., Saragi, I. R., Pamungkas, A.Z., Pratama, A.P. (2021). The new challenge of partial oxidation of methane over Fe$_2$O$_3$/NaY and Fe$_3$O$_4$/NaY heterogeneous catalysts. *Heliyon*, 7 (11), 0–7, DOI: 10.1016/j.heliyon.2021.e08305.

[37] Kosinov, N., Coumans, F.J.A.G., Li, G., Uslamin, E., Mezari, B., Wijpkema, A.S.G., Pidko, E.A., Hensen, E.J.M. (2017). Stable Mo/HZSM-5 methane dehydroaromatization catalysts optimized for high-temperature calcination-regeneration. *J. Catal.*, 346, 125–133, DOI: 10.1016/j.jcat.2016.12.006.

[38] Abdelsayed, V., Smith, M.W., Shekhawat, D. (2015). Investigation of the stability of Zn-based HZSM-5 catalysts for methane dehydroaromatization. *Appl. Catal. A Gen.*, 505, 365–374, DOI: 10.1016/j.apcata.2015.08.017.

[39] Lónyi, F., Valyon, J. (2001), On the interpretation of the NH$_3$-TPD patterns of H-ZSM-5 and H-mordenite, *Microporous Mesoporous Mater.*, 47 (2–3), 293–301. DOI: 10.1016/s1387-1811(01)00389-4

[40] Wei, Z., Chen, l., Cao, Q., Wen, Z., Zhou, Z., Xu, Y., Zhu, X. (2017). Steamed Zn/ZSM-5 catalysts for improved methanol aromatization with high stability, *Fuel Process. Technol.*, 162 (66–77), DOI: 10.1016/j.fuproc.2017.03.026.

[41] Liu, C., Wang, H., Karim, A.M., Sun, J., Wang, Y. (2014). Catalytic fast pyrolysis of lignocellulosic biomass. *Chem. Soc. Rev.*, 43 (22), 7594–7623, DOI: 10.1039/c3cs60414d.

[42] Yao, G., Wu, G., Dai, W., Guan, N., Li, L. (2015), Hydrodeoxygenation of lignin-derived phenolic compounds over bi-functional Ru/H-Beta under mild conditions, *Fuel*, 150, 175–183. DOI: 10.1016/j.fuel.2015.02.035.

[43] Zhao, C., Lercher, J.A. (2012), Selective Hydrodeoxygenation of Lignin-Derived Phenolic Monomers and Dimers to Cycloalkanes on Pd/C and HZSM-5 Catalysts, *ChemCatChem*, 4 (1), 64–68, DOI: 10.1002/cctc.201100273.

[44] Guo, M., Peng, J., Yang, Q., Li, C. (2018). Highly Active and Selective RuPd Bimetallic NPs for the Cleavage of the Diphenyl Ether C-O Bond. *ACS Catal.*, 8 (12), 11174–11183, DOI: 10.1021/acscatal.8b03253.

[45] Jiang, L., Guo, H., Li, C., Zhou, P., Zhang, Z. (2019), Selective cleavage of lignin and lignin model compounds without external hydrogen, catalyzed by heterogeneous nickel catalysts, *Chem. Sci.*, 10 (16), 4458–4468, DOI: 10.1039/c9sc00691e.

[46] Zheng, A., Zhao, Z., Chang, S., Huang, Z., Wu, H., Wang, X., He, F., Li, H. (2014). Effect of crystal size of ZSM-5 on the aromatic yield and selectivity from catalytic fast pyrolysis of biomass. *Journal of Molecular Catalysis A: Chemical*, 383-384, 23–30. DOI: 10.1016/j.molcata.2013.11.005.

[47] Denardin, F.G., Perez-Lopez, O.W. (2019). Methane dehydroaromatization over Fe-M/ZSM-5 catalysts (M = Zr, Nb, Mo), *Microporous and Mesoporous Materials,* 295, 109961. DOI: 10.1016/j.micromeso.109961.

[48] Engtrakul, C., Mukarakate, C., Starace, A.K., Magrini, K.A., Rogers, A.K., Yung, M.M. (2015). Effect of ZSM-5 acidity on aromatic product selectivity during upgrading of pine pyrolysis vapors. *Catalysis Today*, 269, 175-181. DOI: 10.1016/j.cattod.2015.10.032.

[49] Amakawa, K., Wang, Y., Kröhnert, J., Schlögl, R., Trunschke, A. (2019), Acid sites on silica-supported molybdenum oxides probed by ammonia adsorption: Experiment and theory, *Molec. Catal.*, 478, 110580, DOI: 10.1016/j.mcat.2019.110580.

[50] Maddi, B., Davidson, S., Job, H., Dagle, R., Guo, M., Gray, M., Ramasamy, K.K. (2020). Production of Gaseous Olefins from Syngas over a Cobalt-HZSM-5 Catalyst. *Catalysis Letters*, 151 (2), 526-537. DOI: 10.1007/s10562-020-03324-7.

[51] Jiang, W., Cao, J.-P., Zhu, C., Xie, T., Zhao, X.-Y., Zhao, M., Bai, H.C. (2021). Selective cleavage of lignin-derived diphenyl ether C-O bond over weakly acidic Ni/Nb$_2$O$_5$ catalyst. *Fuel*, 295, 120635. DOI: 10.1016/j.fuel.2021.120635

[52] Navajas, A., Jim, E., Romero-sarria, F. (2020). Molybdenum Oxide for the Production of Biodiesel from Oil with High Free Fatty Acids Content. *Catalysts*, 10(2), 158. DOI: 10.3390/catal10020158.

[53] Ben, H., Ragauskas, A. J. (2013). Influence of Si/Al Ratio of ZSM-5 Zeolite on the Properties of Lignin Pyrolysis Products. *ACS Sustainable Chemistry & Engineering*, 1(3), 316–324. DOI: 10.1021/sc300074n

[54] Smail, H.A., Rehan, M., Shareef, K.M., Ramli, Z., Nizami, A.S., Gardy, J. (2019). Synthesis of uniform mesoporous zeolite ZSM-5 catalyst for friedel-crafts acylation. *ChemEngineering*, 3 (2), 1–11, DOI: 10.3390/chemengineering3020035.

[55] Gläser, R., Juan Carlos, U.R., Lazaridis, P.A., Fotopoulos, A.P., Karakoulia, S.A., Triantafyllidis, K.S. (2018). Catalytic Fast Pyrolysis of Kraft Lignin With Conventional, Mesoporous and Nanosized ZSM-5 Zeolite for the Production of Alkyl-Phenols and Aromatics. *Front. Chem.* 1, 295, DOI: 10.3389/fchem.2018.00295.

[56] Zhang, W., Oyama, S.T. (1996), In situ laser Raman studies of intermediates in the catalytic oxidation of ethanol over supported molybdenum oxide, *J. Phys. Chem.,* 100 (25)*,* 10759–10767, DOI: 10.1021/jp960917d